Improving PID-Control of AMB-Rotor System Design II: Experimental Results

Chunsheng Wei*
University of Duisburg-Essen
Duisburg, NRW, Germany

Dirk Söffker
University of Duisburg-Essen
Duisburg, NRW, Germany

Abstract

Most of the industial active magnetic bearings (AMBs) are controlled by PID-Controllers. Usually a time-consuming trial and error procedure is involed to design those PID-Controllers. In part I of this contribution an optimization strategy is introduced to design a complex PID-Controller structure of higher order to be applied on an industrial AMB system. For validation purposes, the selected optimal controllers obtained by using an optimization strategy are applied to a test-rig with a flexible rotor supported by AMBs. In part I of the contribution the control algorithm parameters are optimized, in this part II, the resulting control is implemented on a Digital Signal Processor (DSP) controlling the AMB-rotor system. In combination with a test-rig experiments are performed. Within this contribution various aspects of the implementation are discussed; results are shown.

1 Introduction

Due to their advantages in comparison to conventional bearings, such as contact-free, lubricant-free, etc. active magnetic bearings (AMB) have been received more and more attention in industry area. They are widely used in successful applications in rotor systems, e.g. turbo-compressors [BD02], machine tool spindles, and energy storage flywheel systems.

For an AMB system, the inherent negative stiffness causes instability of the open loop of the system; therefore, a feedback control loop is necessarily employed to stabilize the rotor system. Because of their simple structure and transparent design, PID-controllers are usually selected to control AMB systems in industry applications [PRv+05]. Usually a trial and error procedure is applied to fulfill different criteria of the complex design procedure. Here mainly stability oriented criteria in combination with further desired goals with respect to achieving good performance criteria have to be considered. In part I of the contribution an optimization strategy is presented to design a PID-controller to be applied for AMB systems. This part II of the contribution is focused on the realization of the selected "optimal" PID-controllers to show the validity of the optimization results. Therefore simulation and experimental results are given and compared. The optimal controller is applied to a test-rig with a flexible rotor supported by AMBs. DSP control is for years the standard for industrial AMB systems [BGH+94]. In this paper the control algorithm is implemented on the DSP. The results show that the introduced optimization procedure realizes the desired results of the controlled system's behavior. The whole contribution shows that the controller design of AMB supported flexible rotor can be more effective realized using a suitable design.

This paper is organized as follows: In Section 2 the test-rig introduced. In Section 3 the results of modal analysis are summarized, in Section 4 the detailed experimental results concerning the performance of the selected controller candidates are presented. Finally, a summary is given in Section 5.

*Contact Author Information: E-mail: Chunsheng.wei@uni-due.de; Address: University of Duisburg-Essen, Chair of Dynamics and Control, Lotharstr. 1-21, 47057 Duisburg, Germany; Phone: +49 (0) 203 / 379 - 15 80; Fax: +49 (0) 203 / 3 79 - 30 27

2 Test-Rig

In this section the used test-rig will be briefly described. The test-rig including the driving motor, the gear box, the coupling, and the controller box is shown in Figure 1. The rotor system is driven by a DC (Direct Current) motor (P = 100 kW) with a nominal speed of 2000 rpm. The step up gear is used to increase the speed of the test rotor to the maximal rotational speed of 15000 rpm.

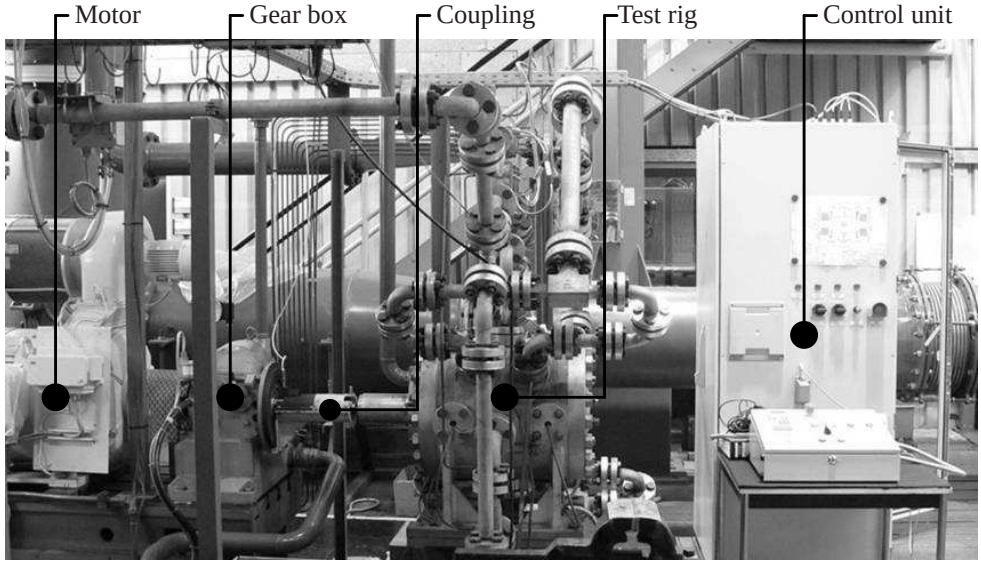

Figure 1: Test rig

The test rotor (steel, geometry of the rotor is given in part I of the contribution) is connected with the driving rotor using a coupling.

The control algorithm is implemented and operated on the DSP unit in the control unit. A communication tool with a Graphical User Interface (GUI) between a PC and the DSP unit is used for data acquisition and parameter modification of the DSP unit. Various functions (e.g. step response, measurement of transfer functions of the AMB-rotor system) can be performed with this communication tool.

In addition to the pair of active magnetic bearings, two auxiliary bearings are arranged at both ends of the test rotor, which are ball-bearings. In normal case (i.e. the magnetic bearing is active), there is no contact between the test rotor and the auxillary bearings. The auxiliary bearings work only when the magnetic bearing is defect (emergency case).

3 Model Validation

In this section, modal analysis of the test rotor is discussed. The tranfer functions of the plant are measured and compared with the simulation results.

3.1 Modal Analysis

An impact hammer modal testing is performed with 27 measure nodes. The eigenfrequencies and eigenforms are calculated. In Table 1 the eigenfrequencies of the modal analysis are summarized. It can be seen that the first two eigenfrequencies (bending mode) are consistent with those result-

Eigenmode	Modal analysis	Simulation	
		0 rpm	15000 rpm
1st bending mode [Hz]	124	117	102/134
2nd bending mode [Hz]	429	419	311/557
3rd bending mode [Hz]	992	942	898/992

Table 1: Comparison of eigenfrequencies from modal analysis and simulation

ing form simulation. The eigenfrequencies obtained from simulation are slightly less than those obtained from modal analysis.

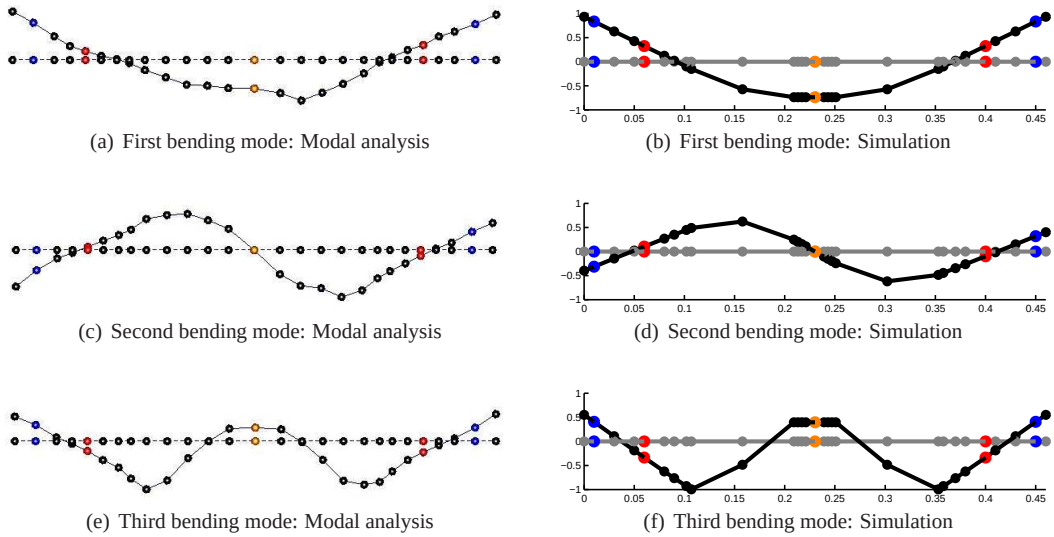

(a) First bending mode: Modal analysis (b) First bending mode: Simulation

(c) Second bending mode: Modal analysis (d) Second bending mode: Simulation

(e) Third bending mode: Modal analysis (f) Third bending mode: Simulation

Figure 2: Comparison of eigenmodes from modal analysis and simulation

The eigenforms of the modal analysis are shown in Figure 2 with 27 nodes. The nodes marked as blue, red, and orange denote the sensor nodes, bearing nodes, and rotor-mid nodes, respectively. The results match quite well with the simulation results.

3.2 Transfer Functions of the Plant

The tranfer functions (including parallel and tilting mode) of the plant are measured from 5 to 2000 Hz. The measurements are performed with the test rotor at rest. The results show the effect caused by the connected driving rotor. In Figure 3 the measured transfer functions of the parallel mode are shown in form of bode diagram. Without the coupling between the test rotor and the driving

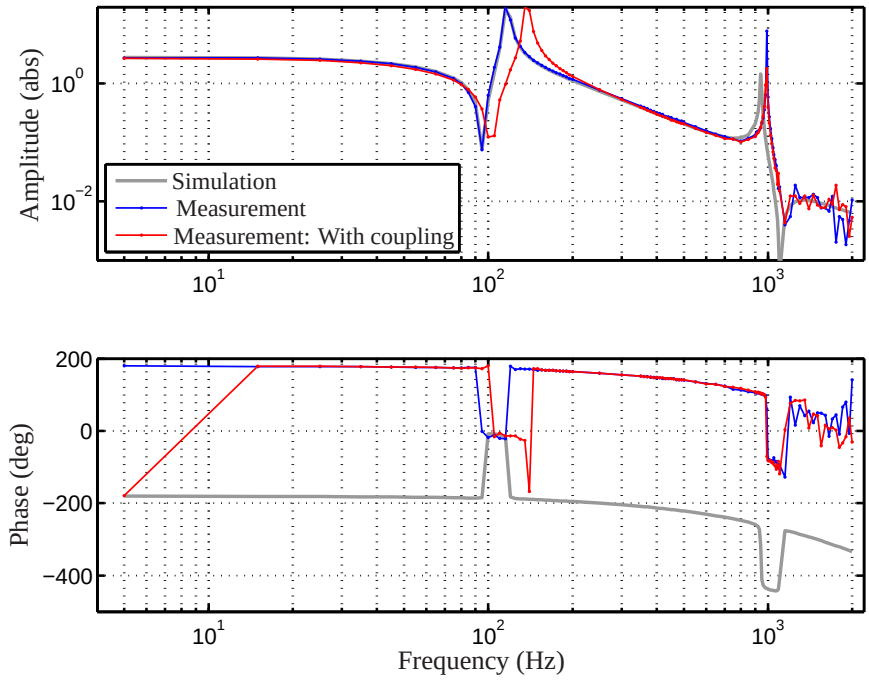

Figure 3: Bode diagram of the plant for parallel mode

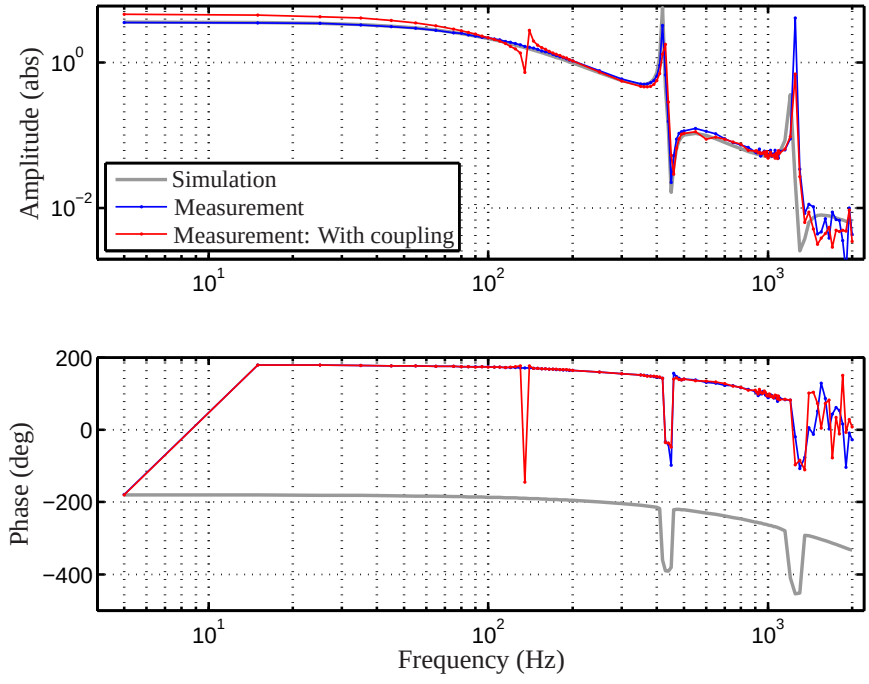

Figure 4: Bode diagram of the plant for tilting mode

rotor (see gray and blue curves), the AMB-rotor system is accurately modeled with respect to the stationary behavior in frequency domain using transfer functions. The dynamics of the test rotor has been strongly influenced by the driving rotor. The eigenfrequency of the first bending mode is shifted to 140 Hz due to the coupling with the driving rotor (see the red curve in Figure 3). Obviously the same situation occurs in the case of the tilting mode as shown in Figure 4. The DC-gain of the plant of tilting mode increases about 28% compared the case without coupling, meanwhile the first bending mode arises in the case of tilting mode due to asymmetry of the test rotor caused by the coupling. For the dynamics at high frequencies, the influence of the coupling is neglected. The effect caused by the coupling changes the performance (e.g. sensitivity) of the selected controller candidates which is based on the model of the test rotor without coupling. The results will be given in the next Section.

4 Performance Evalutation

In this section, the selected two controller candidates obtained by the suggested optimization strategy from the first part of the contribution are compared based on the experimental results consisting of the singular values of sensitivity functions as well as the obtained step responses. Finally an unbalance vibration response is measured up to the maximal rotational speed (15000 rpm) of the rotor.

4.1 Sensitivity

Due to existence of uncertainties and nonlinearities of an AMB-rotor system, the robustness of the closed-loop becomes an essential requirement. The maximal singular value of the sensitivity function gives a robustness measure. According to ISO Stardard 14839-3, a maximal singular value

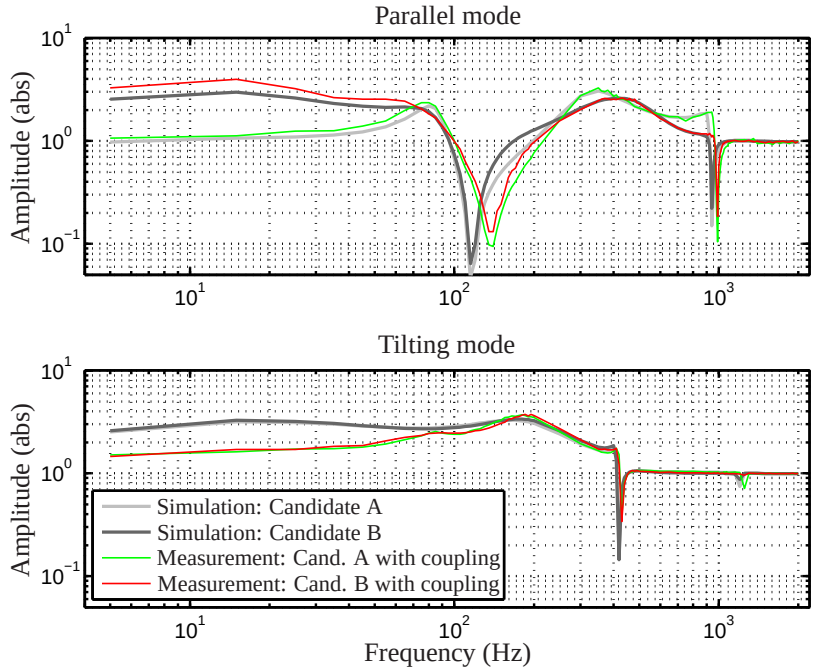

Figure 5: Comparison of the sensitivity from measurement and simulation

shall be less than 4 (A/B zone) for a long term operation of a rotor system supported by AMBs in turbomachinery field.

The sensitivity function is measured for parallel and tilting mode of the AMB-rotor system. The results are shown in Figure 5. For the parallel mode the system with candidate A (green curve) is obviously superior in comparison to the one with candidate B (red curve) as also indicated by the simulation results. The measured maximal singular value of parallel mode is about 3.3 for candidate A and 4.0 for candidate B. Due to the effect of the coupling mentioned in last Section, the position of the first valley of the sensitivity funtion is shifted from 115 Hz to 138 Hz. Comparing the simulation results (no effect of the coupling is considered) with those from the measurement (for the test rotor coupled with the driving rotor), the influence of the coupling for tilting mode is significant at low frequency region. The measured maximal singular value for tilting mode is about 3.7 at the frequency of around 200 Hz.

4.2 Step Response

Step responses are performed and the results are measured and shown in Figure 6. The step starts at t = 0.05 second with a final amplitude value of 50 DSP unit ($\approx 5\ \mu$m). As shown in Figure 6, the

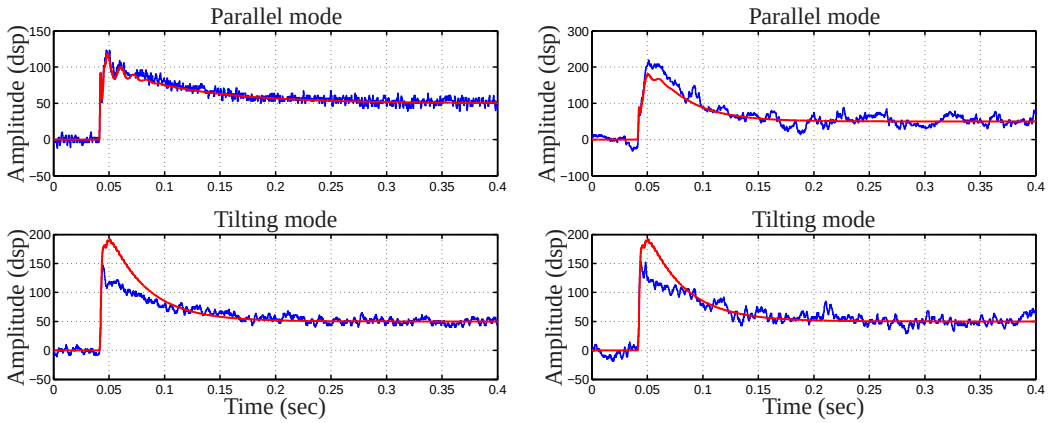

(a) Candidate A (b) Candidate B

Figure 6: Step response from measurement (blue) and simulation (red)

simulated step responses for parallel mode are consistent with the result obtained by measurements. According to this result, it can be concluded that the performance controller candidate A is better than B (smaller overshoot and error). For tilting mode the experimental result has a lower overshoot than those from the simulation. The control current from the step response of parallel mode is shown in Figure 7. It can be seen that the controller candidate A reacts stronger (but more noise occurs) on the controller error (as a result of higher K_P value, see the first part of the contribution) than the controller candidate B, e.g. the peak value of the control current is 0.5 A in case of candidate A and only 0.25 A in case of candidate B.

4.3 Unbalance Vibration Response

The measurement is carried out for the unbalance vibration response from 500 rpm to 15000 rpm. For each rotational speed, the peak-to-peak vibration amplitude is determined. The result is presented in Figure 8. The critical speeds can be easily found from Figure 8, which correspond with the

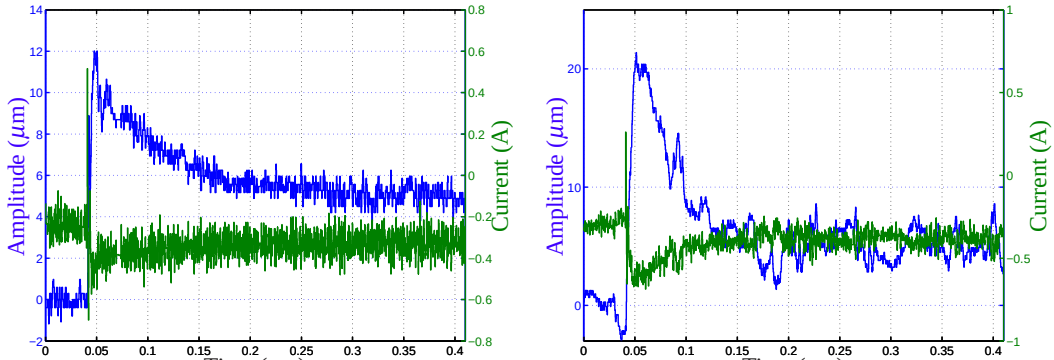

(a) Candidate A (b) Candidate B

Figure 7: Control current for the controller candidate A and B

parallel mode, the tilting mode, and the first bending mode. The peak-to-peak vibration amplitude has a maximal value under 50 μm up to the maximal rotational speed. In Figure 9 the orbit of the rotor for the two sensor nodes (left plot: NDE, right plot: DE) at the rotational speed of 15000 rpm is illustrated. The both orbits are neither elliptic nor circular.

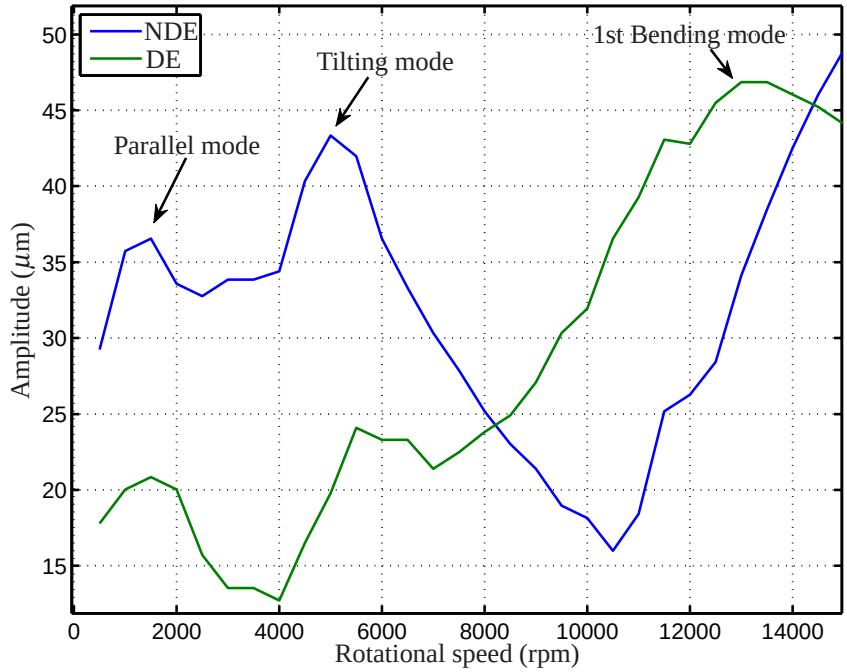

Figure 8: Unbalance vibration response

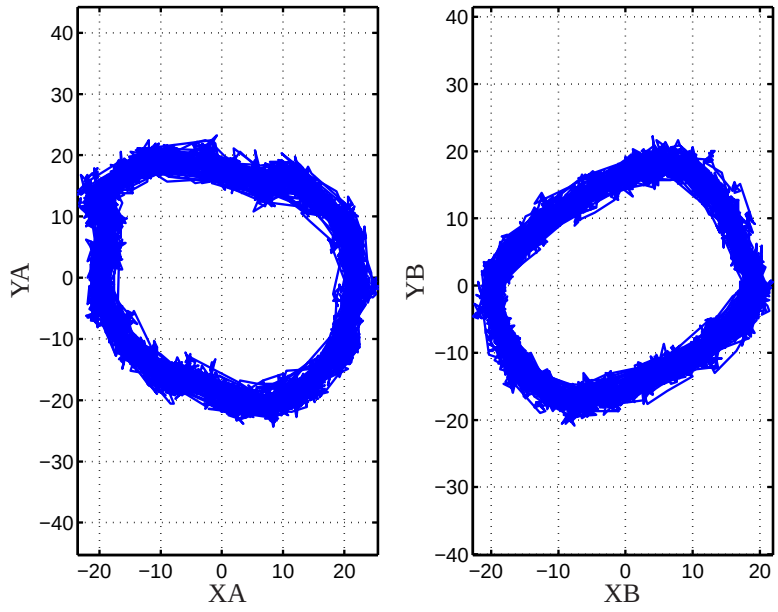

Figure 9: Orbit of the rotor at the rotational speed of 15000 rpm

5 Summary

This paper presents the expmerimental results to validate the optimized controllers by using the suggested optimization approach developed and introduced in part I of the contribution. The results shows that the simulation results match the experimental results in case that the test rotor is not connected with the driving rotor. Otherwise, the dynamics of the AMB-rotor system at low frequencies is changed due to the coupling used to connect the test rotor with the driving rotor. The controller candidate A gives a good performance (small maximal singlular value, low overshoot, small vibration amplitude through the whole rotation region). It can be seen that the complex PID-Controller for AMB-rotor system can be determined and optimized by using the introduced optimization strategy.

References

[BD02] M. Brunet and Y. Destombes. Application of active magnetic bearings in turbocompressors and turboexpanders of the gas industry. *Chemical and Petroleum Engineering*, 38(7-8):459–463, 2002.

[BGH+94] H. Bleuler, C. Gähler, R. Herzog, R. Larsonneur, T. Mizuno, R. Siegwart, and S.J. Woo. Application of digital signal processors for industrial magnetic bearings. *IEEE Transaction on Control Systems Technology*, 2(4):280–289, 1994.

[PRv+05] B Polajžer, J Ritonja, G Štumberger, D Dolinar, and J P Lecointe. Decentralized pi/pd position control for active magnetic bearings. *Electrical Engineering*, 89(1):53–59, 2005.